

Investigation of the mechanism of energy dissipation in the front of a turbulent electrostatic shock wave

N. V. Astrakhantsev, O. L. Volkov, V. G. Eselevich, G. N. Kichigin, and V. L. Papernyi

Siberian Institute of Terrestrial Magnetism, Ionosphere and Radiowave Propagation, Academy of Sciences USSR

(Submitted 20 February 1978)

Zh. Eksp. Teor. Fiz. **75**, 1289-1302 (October 1978)

The nature of turbulent processes and the mechanism of collisionless energy dissipation in the front of an electrostatic turbulent shock wave due to them are studied experimentally. It is shown that the development of instability of opposing ion beams results in a high level of turbulent noise, $W/nT_e \leq 0.2$ in the shock wave. The scattering of incident plasma ions by this noise is a mechanism which ensures beam energy dissipation over a distance of twenty Debye lengths. A phenomenological shock wave model is proposed which is based on two-stream electrostatic ion instability.

PACS numbers: 52.35.Tc, 52.35.Ra, 52.35.Fp, 52.40.Mj

I. INTRODUCTION

A turbulent electrostatic shock wave with Mach number $M = u/c_s \approx 2-3$ was discovered in experiments^{1,2} on the interaction of the flow of a rarefield nonisothermal plasma ($T_e \gg T_i$) with a magnetic "barrier" (u is the velocity of plasma flow, c_s is the ion sound velocity). The width of the shock front amounted to several centimeters, which is 2-3 orders smaller than the free path length of the particles of the plasma relative to pair collisions. The formation of a collisionless shock front was attributed to instability development brought about by the part of the flow reflected from the barrier.

The aim of the present work is the study of the nature of the turbulent processes and the character of the dissipation mechanism due to them in the front of an electrostatic turbulent shock wave. The study of the mechanism of dissipation in shockwaves of such a type is of general physical and applied interest, since similar effects can play a decisive role in such phenomena as an earth surface shock wave,³ isomagnetic discontinuities in the form shock wave front in magnetized plasma,⁴ the interaction of ion beams with a plasma target,⁵ and so on.

The study of processes in the front of an electrostatic turbulent wave has been carried out in two directions: 1) the study of macroscopic density distributions and distribution of potential and flow velocity of the ions, and also the spectrum of random electrostatic oscillations, time and amplitude characteristics, which makes it possible to establish the nature of the turbulent processes; 2) the study of the distribution function of the ions and ahead and behind the front, which enables us to decide on the character of the dissipation mechanism.

II. APPARATUS AND METHOD OF DIAGNOSTICS

1. The experiments were carried out on the "SOMB" apparatus.^{1,2} The diagram of the apparatus is shown in Fig. 1. The plasma flow was created in a metallic vacuum chamber having the shape of a cylinder of length (L) 200 cm, diameter (D) 60 cm. A pulse of the working gas (argon) was let into the volume, which has been pumped down to a pressure of $\leq 5 \times 10^{-6}$ Torr, from one of the ends, making the pressure in the region of the ionizer $\approx 10^{-4}$ Torr. The expanding cloud was ionized by the current of electrons accelerated from the heated cathode. The plasma that was formed spread out in the vacuum at a velocity $u \approx (5 \times 10^5 - 10^6)$ cm/sec along the x axis of the volume, much greater than the velocity of motion of the boundary of the neutral gas, $\leq 10^4$ cm/sec. Within a time of 10^{-4} sec, a quasistationary flow of plasma was established in the region of the magnetic "barrier," located at a distance of 100 cm from the ion-

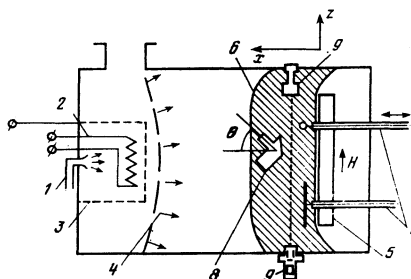


FIG. 1. Diagram of the experimental setup: 1—pulsed valve for letting in the gas; 2—heated cathode; 3—wire-gauze anode; 4—front of the neutral gas; 5—solenoid; 6—front of the shock wave; 7—Langmuir probes; 8—Hughes-Rojansky analyzer; 9—apparatus for probing the plasma by a beam of ions.

izer, and lasted 500 μ sec (when the basic measurements were carried out), at a pressure of neutral atoms of $<5 \times 10^{-6}$ Torr. Typical parameters of the plasma flow are the following: density $n_0 \approx 10^6 - 10^8$ cm $^{-3}$, electron temperature $T_e \approx 3 - 5$ eV, ion temperature $T_i \approx 0.1 - 0.3$ eV, diameter (in the limits of which n_0 does not change by more than 10%) about 50 cm. The mean free path of the electrons and ions was determined by collisions with neutral atoms and amounted to $\lambda > 10^3$ cm ($\lambda \gg L, D$). The magnetic "barrier" was produced by a solenoid of rectangular cross section, with dimensions along the coordinate axes (see Fig. 1) $\Delta x = 1.5$ cm, $\Delta u = 15$ cm, $\Delta z = 40$ cm, coil spacing 1 cm and diameter of the wire 0.1 cm. The magnetic field $H_{p0} \leq 400$ Oe is essentially concentrated inside the solenoid, such that the field at a distance $|x| > 1.5$ cm from the wire is less than $10^{-2} H_{p0}$.

2. Langmuir probes—cylindrical (diameter $d = 0.03$, length $l_p = 20$ cm) and spherical (diameter $d_s = 0.6$ cm)—were used for measurement of the electron temperature, density and directed velocity of the plasma current, and also the parameters of oscillations in the plasma.

In our case of a rarefied collisionless plasma, in which the probe radius is close to (or less than) the Debye radius, the quasistationary current at the probe, as measurements have shown,² is described by the formulas of orbital theory.⁶ The mean velocity of the electrons and ions of the flow were determined from the saturation current of the cylindrical probe $I_{ce,i}$, which, under the condition $|e\Phi| \gg (E_{kin}, T_e)$ (Φ is the potential of the probe relative to the potential of the plasma, $E_{kin} = m_i u^2/2$ is the kinetic energy of the ions of the flow) is connected with $n_{e,i}$ by the relation

$$I_{ce,i} \approx dl_p e n_{e,i} (2e|\Phi|/m_{e,i})^{1/2}. \quad (1)$$

To decrease the perturbing action of the probe on the plasma, the basic measurements were carried out on the ion branch of the probe characteristics.

The time resolution of the probe in the measurement of the oscillation parameters was determined in practice by the time of restructuring the perturbed region around the probe under the action of oscillation in the plasma. Special measurements and estimates showed that significant distortions of the frequency characteristics of the recorded oscillations appear under our experimental conditions at frequencies about $(1-2)\omega_{pi}/2\pi$ ($\omega_{pi}^2 = 4\pi n e^2/m_i$).

The autocorrelation function (ACF) of the oscillations $F(\tau)$ was obtained by analysis of the signal of the Langmuir probe on a high speed computer according to the formula

$$F(\tau) = \left(\int_0^{t_0} I_i(t) I_i(t+\tau) dt \right) / \int_0^{t_0} I_i^2(t) dt, \quad (2)$$

where $\tilde{I}_i(t)$ is the high-frequency component of the probe current, t_0 (≈ 500 μ sec) is the time interval (denoted by the arrows in Fig. 2), during which the oscillation parameters (characteristic frequency, mean amplitude) changed relatively little. By application of the Fourier transformation to $F(\tau)$ we obtained the power spectrum of the oscillations.

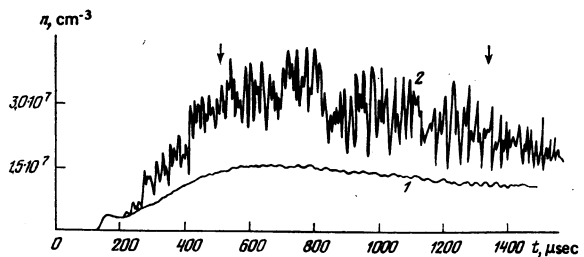


FIG. 2. Oscillograms of the ion current on the probe at a distance of $x = 10$ cm from the "barrier": 1— $H = 0$, 2— $H = 300$ Oe.

The relative energy density of the ion Langmuir oscillations, generated under the conditions of our experiment (see Sec. IV),

$$\epsilon = \frac{W}{nT_e} = \frac{1}{8\pi nT_e} \sum_k |E_k|^2 \approx \frac{k_0^2 \bar{\varphi}^2}{8\pi nT_e}, \quad (3)$$

($\bar{\varphi}$ is the amplitude of the oscillations of the potential with characteristic wave number $k_0 \gg r_D^{-1} = (4\pi n e^2/T_e)^{1/2}$ and frequency ω) was estimated from the measured value of \tilde{I}_i/I_i , which is essentially determined at small values of the oscillations of the ion current $\tilde{I}_i/I_i \ll 1$ by the density oscillations:

$$\tilde{I}_i/I_i \approx \tilde{n}_i/n_i. \quad (4)$$

We find the value of these oscillations from the linearized equations of motion and continuity for the ions (see, for example, Ref. 7, p. 153):

$$\frac{\tilde{n}_i}{n_i} = \frac{k_0 v_i}{\omega - k_0 u} = \frac{e}{m_i} \frac{k_0^2 \bar{\varphi}}{(\omega - k_0 u)^2}. \quad (5)$$

Taking it into account that $\omega - k_0 \cdot u \approx \omega_{pi}$ in the considered oscillations, and using (for estimates) the quasineutrality condition $\hat{n}_e \approx \hat{n}_i = n_e \bar{\varphi}/T_e$ at $k_0 \sim r_D^{-1}$, we get from (3), (4) and (5):

$$\epsilon \sim (I_i/I_i)^2. \quad (6)$$

This relation is valid under conditions in which the length of the probe is small in comparison with the characteristic wavelength of the oscillations λ_0 . Under the conditions of our experiment, to obtain good spatial resolution along the x axis (see Fig. 1), we used thin cylindrical probes oriented along the z axis. To assure the necessary sensitivity the probes had a large length ($l_p = 20$ cm), so that the inverse relation $l_p \gg \lambda_0$ was valid for them. In this case ϵ is undervalued because of averaging of the oscillations over the length of the probe. The wave vector of these oscillations has a component along the probe axis. If the oscillations have a random character, we can use the statistical approach, according to which the value of the relative fluctuations of the current \tilde{I}/I is proportional to $I^{-1/2}$ (in analogy with Ref. 7, p. 534), i.e., according to Eq. (1), it is proportional to $l_p^{-1/2}$. Special measurements confirmed the relation $\tilde{I}/I \sim l_p^{-1/2}$. Consequently, it is necessary to introduce a correction factor in the right side of the expression (6), of order $l_p k_0 \approx l_p/r_D$. More rigorous consideration of this effect in the presence of ion Langmuir oscillations in the plasma, with characteristic wave vector $k_0 \gg r_D^{-1}$, the spectrum of which is assumed to be isotropic with width $\Delta k \sim k_0$, leads to a similar result:

$$\varepsilon \approx \frac{1}{6} \frac{\langle I_i^2 \rangle l_p}{I_i^2 r_D} \quad (7)$$

where $\langle \bar{I}_i^2 \rangle$ is the square of the fluctuation ion current at the probe, averaged over the time interval t_0 .

3. The energy density of the electrostatic oscillations was also determined by the method of scattering of ions of the test beam by microfluctuations of the potential. With this aim, a beam of cesium ions (Cs^+) with energy $E_0 = 4$ keV, diameter 0.8 mm, and duration 300 μsec , was introduced in the plasma at a distance $x = 10$ cm from the barrier along the z axis (see Fig. 1), and was recorded on photographic film, at the exit from the plasma. The use of a microchannel plate in the recorder enabled us to make measurements on a beam of low intensity (beam current $\leq 10^{-10}$ A). According to the method described in Ref. 8, the broadening of the beam $\langle \rho^2 \rangle^{1/2}$ after passage through a plasma region of size l in which electrostatic small-scale ($lk_0 \gg 1$) oscillations are excited with a spectrum assumed to be isotropic ($W \sim 4\pi k_0^3 W_k$), is determined by the expression

$$\langle \rho^2 \rangle \approx 3 \frac{Z^2 e^2}{E_0^2} [(L+l)^2 - L^2] \frac{W}{k_0} \quad (8)$$

where E_0 and Z are the energy and the charge of the particles of the beam, L is the distance from the plasma boundary to the recorder, and k_0 is the value of the characteristic wave vector of the oscillations.

4. Measurements of the non-one-dimensional dynamics of the ion distribution function were carried out on analyzers of two types. The analyzer of the transverse velocities enabled us to obtain, in a time $\leq 10^{-4}$, the transverse-velocity distribution function $f_x(v_x)$ of the beam ions, which represents the transverse cross-section, in velocity space, of a total two-dimensional (say, in the v_x, v_y plane) distribution function of the form $f(v_x, v_y) \approx f_x(v_x - u) f_y(v_y)$ at the point of maximum f_x (at $v_x = u$) under assumption of the smallness of the dispersion of the longitudinal velocities: $\Delta v_x \ll u$.⁹ The distribution function over the "transverse" energy $E_\perp = m_i v_\perp^2 / 2$, which can also be constructed from the signal of the analyzer, we shall denote by $F_\perp(E_\perp)$.

Analyzers of the Hughes-Rojansky type with constant voltage on the plates and a sawtooth voltage (increasing with time) on the diaphragm² made it possible to measure the energy spectrum of the ions $F(E, \theta)$ within a time $\sim 10 \mu\text{sec}$. This function F represents the cross section of the complete distribution function in polar coordinates:

$$f(v_x, v_z) = F(E = m_i(v_x^2 + v_z^2)/2, \quad \theta = \arctg(v_z/v_x))$$

with respect to the angle θ between the axis of the input tube of the analyzer and the direction of the flow velocity (see Fig. 1). The energy resolution of the analyzer $\Delta E/E = 2\%$, the angular resolution $\approx 2.5^\circ$. We used channel electron multipliers (CEM)¹⁰ as recorders in both analyzers. These made it possible to record ion currents with density $n_i v_i \geq 10^{11} \text{ cm}^{-2} \text{ sec}^{-1}$, while the dimensions of the analyzers could be made sufficiently small: $80 \times 10 \times 20$ mm and $80 \times 20 \times 40$ mm, respectively. The analyzers could be oriented at an arbitrary angle θ to the x axis in the xz plane and moved along the x axis.

From the energy spectrum $F(E, \theta)$ obtained experimentally at different angles θ we can construct the distribution function averaged over the components of the velocity transverse to the direction of flow:

$$f(v_x) = \int_{-\infty}^{\infty} f(v_x, v_z) dv_z = v_x \int_{-\pi}^{\pi} F[m_i(v_x^2 + v_z^2)/2, \theta] \frac{d\theta}{\cos^2 \theta} \quad (9)$$

III. EXPERIMENTAL RESULTS

1. Macroscopic characteristics of the shock wave

When a current of a rarefied unmagnetized plasma is incident on a magnetic "barrier", a perturbed zone with intense oscillations is produced. Figure 2 shows an oscillogram of the ion current in the perturbed zone and, for comparison, in unperturbed flow. In Fig. 3c, we have the distribution of the relative level of the oscillations of the ion density along the x axis.

The transition layer (Fig. 3) of width Δ , which separates the perturbed zone from the flowing unperturbed current, surrounds the magnetic barrier and is separated from it by a distance 10–25 cm. This layer is the front of a collisionless shock wave.¹ The basic features of the macroscopic (i.e., averaged over the oscillations) structure of the shock wave are the following: a) a jumplike growth of the ion density, of the potential and of the relative level of the oscillations is noted in the front (Fig. 3); b) the macroscopic structure of the shock wave is practically unchanged during a time $\sim 500 \mu\text{sec}$ which is much larger than the period of the high-frequency oscillations, 10–30 μsec , and the time of flight of the ion of the front, $\Delta/u \leq 10 \mu\text{sec}$, i.e. the wave is quasistationary; c) the width of the front Δ at $M = 2-3$, $T_e = 3-5$ eV, and in the range $n_0 \approx 5 \times (10^8 - 10^9) \text{ cm}^{-3}$, is about $20r_D$ (Fig. 4), that is, it falls off with increase in n_0 approximately like $n_0^{-1/2}$. The quantity Δ remains much less than the length of pair collisions.

A characteristic feature of the wave front structure is the excellent agreement in the profiles of the levels of the oscillations and the density in the foot, and a somewhat greater width in the jump of the levels of oscillations in comparison with the jump in the density.

2. Analysis of turbulence in the shock front in the perturbed zone

The formation of a perturbed zone and a shock wave is connected with the existence of an ion current that is

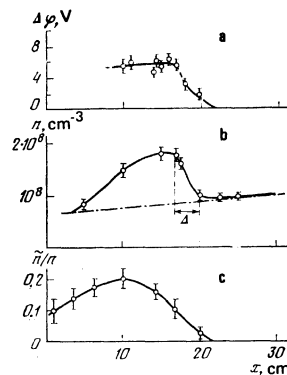


FIG. 3. a—profile of the potential in the perturbed region in front of the "barrier," b—profile of the density, c—profile of the level of oscillations.

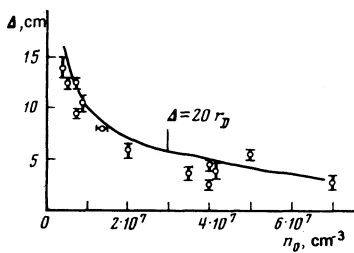


FIG. 4. Dependence of the width of the front on the density of the plasma.

reflected from the magnetic barrier and causes buildup of the oscillations.^{1,2} The relative density of the reflected ions near the barrier is $\alpha = n_{\text{refl}}/n_0 \approx 0.1-0.5$, the velocity is $u_{\text{refl}} \approx -u$, and $T_{i\text{refl}} \approx T_i$.

The instability and character of the oscillations localized in the perturbed zone (Fig. 3c), were studied by using Langmuir probes with correlation analysis. The basic results of the measurements reduce to the following: a) the mean period and amplitude of the oscillations do not change during the interval of time $\sim 500 \mu\text{sec}$; b) the autocorrelation function of the high-frequency component of the probe signal (Fig. 5a), obtained with the aid of relation (2), is damped out even after a single oscillation, while the power spectrum constructed from it (averaged over 20 cases) has a width Δf that is close to the characteristic frequency of the oscillations: $\Delta f \sim f_0 \approx 0.5\omega_{pi}/2\pi$ (see Fig. 5b); the rapid loss of the correlation and the large width of the amplitude-frequency spectrum of the oscillations indicate the existence in the plasma of stochastic turbulent noise; c) an estimate of the established energy level of the noise, made according to formula (7), for typical experimental conditions (see Fig. 2) $\langle \tilde{I}_i^2 \rangle / I_i^2 \approx 10^{-2}$ and $l_p/r_D \approx 60$, gives a value $\epsilon \approx 0.1$.

The absolute value of the level of the turbulence was monitored against the broadening of the diagnostic ion beam. Measurements showed that with broadening of the beam in the absence of turbulence is negligibly small. Figure 6 shows images of the beam, taken at 500 μsec prior to arrival of plasma (a) and 500 μsec after arrival of the plasma in the perturbed zone (b) and also the density distributions of these images in horizontal cross section. It is seen from the drawings that after passage through the turbulent region, the beam was broadened. The broadening of the beam is diffuse and can be attributed to scattering of the particles of the beam by the potential fluctuations whose period is much less than the time of recording. Estimate of the level of turbulence, obtained from Eq. (8), at a broad-

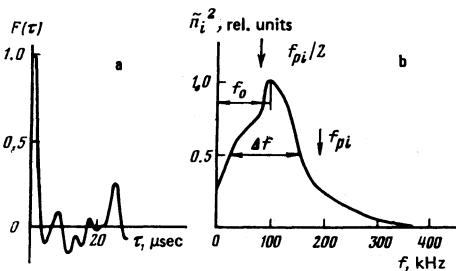


FIG. 5. a—autocorrelation function; b—amplitude-frequency spectrum of the oscillations in the turbulent region.

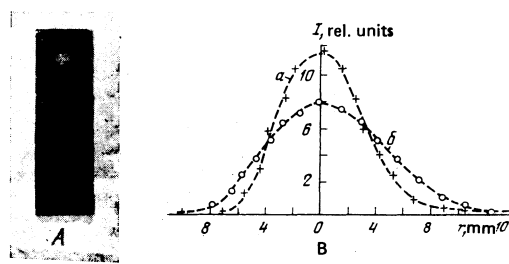


FIG. 6. Image of the ion beam (A) and its photometric density distribution (B): a—500 μsec before the arrival of the plasma; b—500 μsec after arrival of the plasma at the barrier.

ening $\langle \rho^2 \rangle^{1/2} \approx 0.02 \text{ cm}$, $k_0 \approx r_D^{-1} \approx 3 \text{ cm}^{-1}$, and $L \approx 0$, $l \approx 30 \text{ cm}$, gives the value $\epsilon \approx 2 \times 10^{-2}$ —of the same order as that obtained from the probes. A typical value of the established level of turbulence behind the shock front lies in the range $\epsilon = 0.2-0.02$, which is 4–5 order greater than the energy density of thermal noise ($W_T = T_e/2\pi^2 r_D^3$).

The circular shape of the image of the broadened beam supports the assumption that the oscillations are isotropic, at least in the probing region (behind the wavefront). Measurements of the spatial correlation function with the help of probes in this region also did not show the presence of a preferred direction of the oscillations.

3. Investigation of the distribution function of the ions in the turbulent region

The presence of a high level of turbulence in the perturbed zone can lead to a significant change in the distribution function of the incident and reflected currents. For study of this effect by means of the analyzers described in subsection 4 of Sec. II, measurements were made of the ion distribution function in the total energy $F(E, \theta)$ and in the transverse energy $F_1(E_1)$.

The $F_1(E_1)$ dependence of the unperturbed flow is shown in Fig. 7a in a semi-log plot. It is seen from the drawing that the ions distribution function is close to Maxwellian with a transverse temperature $T_{i1} \approx 0.2 \text{ eV}$. After passage of the turbulent front, $F_1(E_1)$ acquires a “tail” of particles accelerated in the transversd direction (Fig. 7b), while the temperature of the bulk of the

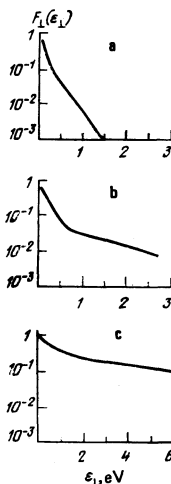


FIG. 7. Distribution function of the ions over the “transverse” energies of the incident (a, b) and reflected (c) streams: a— $x = 25 \text{ cm}$, b— $x = 15 \text{ cm}$, c— $x = 8 \text{ cm}$ from the “barrier” ($H = 300 \text{ Oe}$).

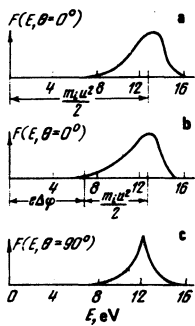


FIG. 8. Energy spectrum of the ions on the incident stream (rel. units) $z = -x = 25$ cm, b and c— $x = 15$ cm, $u_1 =$ velocity of stream behind the wavefront.

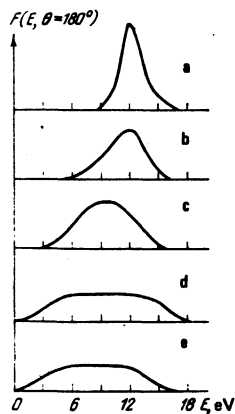


FIG. 10. Energy spectrum of the ions of the reflected stream at distances of (a) 5 cm; (b) 10 cm; (c) 15 cm; (d) 20 cm; (e) 25 cm from the "barrier."

ions remains almost unchanged. Upon further motion of the flow toward the "barrier", the shape of $F_{\perp}(E_{\perp})$ changes comparatively little. Measurements of $F_{\perp}(E_{\perp})$ of the reflected flow have shown that an increase in the "effective" transverse temperature of the ions takes place already at distances less than 8 cm from the "barrier," to a value $T_{i\perp} \approx 3$ eV, which is close to the electron temperature (see Fig. 7c). In further motion ($x > 8$ cm) from the barrier, the "transverse" distribution function of the reflected ions changes little.

The study by means of a Hughes-Rojansky analyzer of the energy spectrum of the main-stream ions moving along the x axis, $F(E, \theta = 0)$ showed that on passage of the shock front, electrostatic retardation of these ions takes place with weak distortion of the shape of the spectrum $F(E, \theta = 0)$. (See Fig. 8a, b). At the same time ions appear behind the front, moving at large angles θ to the direction of motion of the flow. It follows from the shape of the energy spectrum of these ions, shown in Fig. 8c, that they appeared as a result of almost elastic scattering of the particles of the incident flow from oscillations in the region of the front (the change in the modulus of the ion velocity by the scattering does not exceed 10% and lies within the limits of experimental error). We note here a characteristic decrease in the width ("sharpening") of the spectrum of the scattered particles. The angular distribution of maxima of the spectra $F(E = 13 \text{ eV}, \theta)$ and of the density of particles $dn/d\theta$ are given in Fig. 9, from which it follows that the scattering with respect to angle has a diffuse character (an increase in density near $\theta = 180^\circ$ corresponds to reflected flow).

The energy spectrum of the ions of reflected flow $F(E, \theta = 180^\circ)$ near the "barrier" is similar to the spectrum of the incident flow (see Fig. 10a). As the distance from the "barrier" increases, a comparatively slow—over the extent of the entire turbulent zone $x < 20$ cm—broadening of the spectrum in the direction of lower energy takes place (see Figs. 10b, c, d). The shape

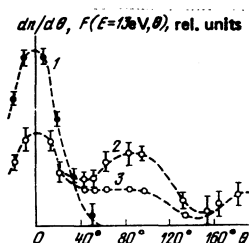


FIG. 9. Angular distribution of the maxima of the spectra: 1— $x = 25$ cm; 2— $x = 15$ cm; 3—angular distribution of the density $dn_i/d\theta$ ($x = 15$ cm).

of the spectrum of the reflected ions is practically unchanged after emergence from the turbulent region (Fig. 10e). These data attest to the inelastic (with energy loss) character of the interaction of the turbulent oscillations with the ions of the less dense reflected stream. The ion distribution function of the reflected stream over the longitudinal velocities $f(v)$ in the turbulent zone and in the unperturbed flow, constructed from measurements of $F(E, \theta)$ (see Eq. (9)), has the shape shown in Fig. 11. It follows from the drawing that the directed velocity of the ion flow after passage of the shock front, decreases by a factor of about two, while the effective longitudinal temperature of the ions of the slowly rises from $T_i = 0.2$ eV ahead of the front to $T_i = 1$ eV behind it.

The introduction of the analyzers into the shock wave, as results of measurements by Langmuir probes have shown, has no effect on its macroscopic structure and on the parameters of the turbulence.

The measurement of the temperature of the electron component was carried out with the help of standard probe methods. The change in T_e in the shock front is within the limits of accuracy of the measurements, which, under our conditions of a turbulent plasma, amounted to about 30%.

IV. DISCUSSION OF RESULTS

On the basis of the experimental results, the following qualitative picture of the formation of a turbulent shock wave can be considered. As a result of the de-

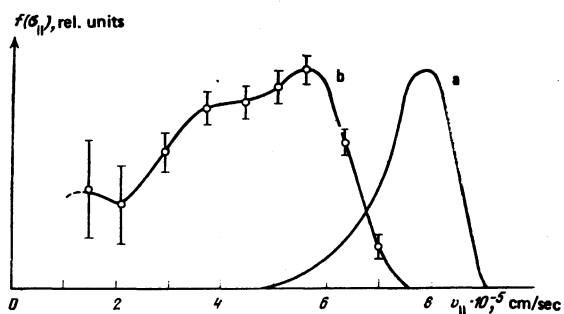


FIG. 11. Distribution function of the ions of the incident stream, integrated over the transverse velocities: a—ahead of the front; b—behind the front.

velopment of beam ion instability in front of the "barrier," a turbulence zone arises with a high level of oscillations. The ions of the supersonic flow of the plasma, flowing into the turbulence zone, are scattered by the microfluctuations of the potential. This scattering leads to an increase in the dispersion of the velocities of the ions of the flow (i.e., to effective "heating") and to a broadening of the distribution function towards the lower energies (i.e., a retardation of the flow). This indicates the presence of collisionless dissipation of the energy of the directed motion of the flow. In turn, the decrease in the velocity leads to an increase in the density and the potential on the boundary of the turbulence region. In further motion in the direction of the "barrier," part of the flow ions, being scattered at large angles, leave the turbulence region (which has finite transverse dimensions); this can explain the observed decrease in the density behind the front in the direction of the "barrier" (see Fig. 3a).

The experimentally observed features of the interaction of the flow ions with the oscillations can be obtained from a consideration of a phenomenological model of a turbulent shock wave. Within the framework of this model, we shall make, with respect to the character of the oscillations and the structure of the turbulence region, assumptions that do not contradict the experimental data, and obtain the dynamics of the distribution function of the flow ions by a qualitative analysis of the quasilinear equations. We also clarify the conditions of formation of the macroscopic structure of the wavefront.

We shall assume that:

1. When a supersonic stream of nonisothermal plasma is incident on a magnetic "barrier," with velocity $u \gg c_s$, a small part of the flow ions ($\alpha = n_{\text{refl}}/n_0 \ll 1$) are reflected from the barrier and, moving against the original flow, cause buildup of ion-ion instability. Since the relative velocity of the beam in the plasma is $v_{\text{rel}} \approx 2u \gg c_s$, the branch of ion Langmuir oscillations builds up at a maximum increment with a characteristic frequency $\approx \omega_{pi}$ (in the system of the fundamental, more dense stream) and with wave vector $k_0 \approx r_D^{-1}$ directed at an angle $\theta \approx \arccos(c_s/v_{\text{rel}})$ to the vector of the beam velocity.¹¹ We obtain the frequency of the oscillations in the laboratory system of coordinates ω with account of the drift in the main stream of the plasma with velocity \mathbf{u} , i.e., according to the formula of the Doppler shift, $\omega \approx \omega_{pi} = \mathbf{k} \cdot \mathbf{u}$. From the condition of resonance buildup of the oscillations by the weak reflected beam, moving with velocity $\mathbf{u}_{\text{refl}} \approx -\mathbf{u}$, $\omega \approx \mathbf{k} \cdot \mathbf{u}_{\text{refl}} = -\mathbf{k} \cdot \mathbf{u}$ we find $\omega \approx \omega_{pi}/2$ (see Figs. 5 and 6).

2. In the region of the front, the oscillations come out of the resonance with the diffuse ($(\Delta u/u)_{\text{refl}} \gg \alpha^{1/3}$) beam. Their group velocity in the system of coordinates of the denser plasma stream is $\leq c_s$. Therefore, the group velocity of the oscillations in the laboratory system of coordinates is $\approx u$ because of the dragging by the supersonic flow of the plasma in the direction of the "barrier" with velocity $u \gg c_s$ (which is valid, strictly speaking, only at the base of the front). As a consequence of this, formation of a localized region with a

high level of turbulent noise occurs in front of the "barrier."

3. The density of noise energy $W_n(x)$ depends on the coordinate x in the direction of motion of the flow and changes materially only in the front, whose dimension is $\Delta \gg k_0^{-1} \approx r_D$, and changes little outside of it (see Fig. 3c).

The evolution of the distribution function $f(\mathbf{v}, x)$ of the ions of the flow which we also assume to depend only on the x coordinate, is described by the stationary quasilinear equation

$$v_x \frac{\partial f}{\partial x} - \frac{e}{m} \frac{\partial \Phi}{\partial x} \frac{\partial f}{\partial v_x} = \frac{\partial}{\partial v_i} D_{ij} \frac{\partial f}{\partial v_j}, \quad (10)$$

where $\Phi(x)$ is the mean potential and D_{ij} is a nonresonant diffusion coefficient. Using the stationary kinetic equation for waves in an inhomogeneous plasma with account of condition 2, we can show that the nonresonant diffusion coefficient D_{ij} is proportional to $u(\partial W_n/\partial x)$.¹² It then follows that diffusion takes place mainly in the transition layer at the boundary of the turbulent region, where the noise level changes significantly although the size of the entire region can exceed the width of the layer by an appreciable amount. Therefore, the distribution function of the ions of the basic flow, and, consequently, its moments—the density of the plasma, the directed velocity—also change only in this layer, which is then the front of a turbulent shock wave (see Fig. 3).

The nonresonant diffusion coefficient D_{ij} can be calculated in the spherical coordinates (v, θ, φ) in velocity space and (k, θ', φ') in the space of the wave vectors, with account of the axial symmetry of the problem $\partial/\partial \varphi = \partial/\partial \varphi' = 0$ (the polar angles θ and θ' are measured from an axis perpendicular to the flow velocity vector \mathbf{u}). By virtue of the predominantly transverse direction of the wave vectors of the oscillations (see condition 1), the principal term in the tensor, because of the inequality

$$|\cos \theta'| \approx \frac{c_s}{2u} \ll 1, \quad |\sin \theta| \approx \frac{v_{\text{rel}}}{u} \approx \frac{c_s}{u} \left(\frac{T_1}{T_s} \right)^{1/2} \ll 1 \quad (11)$$

turns out to be the term $D_{\theta\theta}$,¹² which describes the turning of the distribution function [in the diffusion Eq. (10)] through the angle θ with conservation of the velocity modulus. Such a behavior of the distribution function agrees qualitatively with the results of measurements (see Fig. 8) and is analogous to the case of resonance scattering by oscillations of the ions of a fast beam.¹¹ Here, since the diffusion operator contains only angle variables, the right side of Eq. (10) is a maximum at the point $v = u$, where $f(v, \theta, x)$ has a maximum. This means that the particles with maximum angular diffusion are those from the maximum of $f(v, \theta)$, i.e., the width of the spectrum of the scattered particles $F(E, \theta \geq 20^\circ)$ is less than the width of the spectrum of the particles of the initial stream $F(E, \theta = 0)$ (cf. Figs. 8b and c).

We note that the results are valid, strictly speaking, only at the base of the front, where the noise level is sufficiently low and the distribution function of the flow ions did not differ too much from the initial, so that the

inequalities (11) remain in force.

We now make clear under what conditions we can obtain in our model an increase in the mean density of the plasma n in the region of growth of the noise level W , i.e., the tendency to formation of a macroscopic structure of the front. With this aim, we make use of the moment equations for the distribution functions of the ions of the basic flow in the hydrodynamic approximation. This enables us to confine ourselves to the first two moments.

Conservation of flow of matter gives

$$\partial(nu)/\partial x=0. \quad (12)$$

Here $u(x)$ and $n(x)$ are the velocity of flow of the plasma and its density, the contribution to which by ions of the weak reflected beam we have neglected.

The equation for the flow of momentum can be written with account of the fact that the total force exerted on the plasma by the electrostatic oscillations is the gradient, taken with the minus sign, of the energy density of the oscillations,¹³ i.e.,

$$\frac{\partial}{\partial x}(mnu^2+nT_e)=-\frac{\partial W}{\partial x}. \quad (13)$$

In this expression, the term with the electron pressure corresponds to the term which takes into account the mean electric field in the kinetic equation (10) in the quasineutral approximation. We have neglected the contribution of the flow of momentum of the reflected beam of ions in comparison with W .

From Eqs. (12) and (13) we find (at $\delta n/n_0 \ll 1$)

$$\delta n/n_0=(n-n_0)/n_0 \approx W/(M^2-1)n_0T_e, \quad (14)$$

where n_0 is the unperturbed density of the plasma. It follows from this relation that the stationary flow of plasma to the region of localization of the electrostatic oscillations is accompanied by an increase in the density of the plasma only in the case of supersonic flow ($M=u/c_s > 1$). This result is valid for all electrostatic oscillations and does not depend on the shape of their spectrum (which can be, in particular, one-dimensional). However, if the formation of a turbulent region is connected with the development of two-stream ion instability, then the supersonic relative motion of the streams (which, according to (14), is the necessary condition for the appearance of the density discontinuity) leads to an essentially non-one-dimensional character of both the spectrum of the oscillations and of the evolution of the distribution function, in agreement with the results obtained above. In the case of subsonic stream motion accompanied by a one-dimensional spectrum of oscillations,¹¹ a decrease of the plasma density takes place in the region of growth of the noise level, in correspondence with the results of the analysis of the well-known model of Tidman.¹⁴

Thus, a shock front develops on the boundary of the turbulent region, and is due to the interaction of the ions of the plasma flow with the turbulent oscillations. Limiting ourselves to the estimate proposed in Ref. 15, we can express the width of the front Δ in terms of the turbulence parameters:

$$\Delta \sim \frac{1}{k_0 \varepsilon} \left(\frac{m_i u^2}{2T_e} \right)^{1/2}.$$

For $\varepsilon \sim 0.1$, $m_i u^2/2T_e \approx 3$, and $k_0 \approx r_D^{-1}$ we obtain $\Delta \sim 10^2 r_D$, which agrees in order of magnitude with the experimental values. The dependence $\Delta = \Delta(n_0) \sim n_0^{-1/2}$, which follows from this estimate also agrees well with that obtained from experiment (see Fig. 4).

V. CONCLUSION

The results of the experiments have shown the following.

1. The development of two-stream ion instability, which arises upon interaction of a supersonic plasma incident on a magnetic "barrier" with a low-density beam reflected from it, leads to the formation, in front of the "barrier," of a quasistationary turbulent region with oscillations that have an essentially three-dimensional character and a high level ($\varepsilon \leq 0.2$).

2. The interaction of microfields of the oscillations (in the turbulent region) with oppositely moving ion streams takes place in an essentially different fashion: the ions of the denser incident plasma are scattered diffusely from the oscillations, and their velocity modulus changes little, while the ions of the weak reflected flow interact inelastically with the oscillations and experience a significant loss of kinetic energy.

3. The diffuse scattering of the ions of incident plasma ions by the oscillations is a mechanism which guarantees a retardation of the flow and effective heating of the ions in a transition layer of scale $\sim 20r_D$ at the boundary of the turbulent region, which is the front of the turbulent shock wave. Inasmuch as the length of the Coulomb ion-ion collisions is much greater than the width of the shock front, its formation is connected with the appearance of a turbulent ion viscosity.

A phenomenological model of electrostatic turbulence of the shock wave was proposed on the basis of two-stream ion instability. Within the framework of this model, we have obtained of the ions of the incident stream a distribution function which agrees qualitatively with the experimental data, and obtained also a tendency toward the formation of a macroscopic structure of the front. The principal significance of the supersonic flow of the plasma in the front of the wave has been demonstrated, and by the same token the three-dimensional character of the oscillations and of the dynamics of the ion distribution function.

In conclusion, we note several possible applications of the results. The investigation of the earth-surface shock wave with the help of artificial satellites has shown³ that collisionless heating of the ions of the incident solar wind takes place under certain conditions in a narrow layer ("subshock") inside the shock front, which is characterized by a high level of electrostatic noise. The presence of ion streams in this region enables us to attribute the formation of a narrow zone (in which turbulent ion viscosity takes place), to the buildup of two-stream ion instability, and to attribute the narrow layer itself to the turbulent electrostatic shock

front.

In laboratory experiments on collisionless shock waves transverse to the magnetic field at large Mach numbers, the appearance of a discontinuity in the potential and in the density of scale $<100r_D$ is observed; this is much smaller than the thickness of the front—the so-called “isomagnetic discontinuity.”

As a possible mechanism of formation of the discontinuity, the density the dispersion of ion-sound waves was discussed in Ref. 4. Their role is reduced to a limitation of the nonlinear steepening of the density over a scale of the order of tens of Debye lengths. The results of the experiments described above enable us to admit the turbulent ion viscosity as an alternative mechanism of formation of the isomagnetic discontinuity, not only to assure the small size of the discontinuity, but only to explain the energy of the ions in the wave-front observed in this dissipation.

The authors thank I. G. Shukhman for fruitful discussions.

- ¹O. L. Volkov, V. G. Eselevich, G. N. Kichigin and V. L. Papernyi, Zh. Eksp. Teor. Fiz. 67, 1689 (1974) [Sov. Phys. -JETP 40, 841 (1974)].
²O. L. Volkov, V. G. Eselevich, G. N. Kichigin and V. L. Papernyi, Preprint Siberian Inst. Terrest. Magnetism, Ionosphere and Radiowave Propagation, No. 5-74, 1974.
³V. Formisano and C. Hedgcock, J. Geoph. Res. 78, 3705 (1973).

- ⁴A. G. Es'kov, V. G. Eselevich, R. Kh. Kurtmullaev and A. I. Malyutin, Zh. Eksp. Teor. Fiz. 60, 5 (1971) [sic!].
⁵K. B. Kartashev, V. I. Pistunovich, V. V. Platonov, V. D. Ryutov and E. A. Filimonova, Fizika plazmy (1, 742 (1975) [Sov. J. Plasma Phys. 1, 406 (1975)].
⁶F. Chen, translation in: Diagnostika plazmy (Plasma Diagnostics) (R. Huddleston and S. Leonard, eds.) Mir, 1967, p. 107.
⁷Elektrodinamika plazmy (Electrodynamics of plasma) A. I. Akhiezer, ed., Nauka, 1974.
⁸V. S. Koidan, A. G. Ponomarenko, A. I. Rogozin, D. D. Ryutov, in: Diagnostika plazmy (Plasma Diagnostics) No. 3, Atomizdat, 1973.
⁹N. V. Astrakhantsev, V. G. Eselevich, G. N. Kichigin, V. L. Papernyi, Zh. Tekh. Fiz. 48, 297 (1978) [Sov. Phys. Tech. Phys. 23, 178 (1978)].
¹⁰B. M. Glukhovskoi, V. M. Evtikhmeva, I. B. Maksyutov and V. L. Papernyi, Elektronnaya tekhnika, ser. 5, No. 5, 17 (1976).
¹¹A. A. Ivanov, S. I. Krashennikov, T. K. Soboleva, and P. N. Yushmanov, Fiz. Plazmy 1, 753 (1975) [Sov. J. Plasma Phys. 1, 412 (1975)].
¹²N. V. Astrakhantsev, O. L. Volkov, V. G. Eselevich, G. N. Kichigin, V. L. Papernyi and I. G. Shukhman, Preprint, Siberian Inst. Terrest. Magnetism, Ionosphere and Radiowave Propagation, No. 11-77, 1977.
¹³B. B. Kadomtsev, in: Voprosy teorii plazmy (Problems of Plasma Theory) No. 4, Atomizdat, 1964, p. 216.
¹⁴D. Biskamp and D. Pfirsch, Phys. Fluids 12, 732 (1969).
¹⁵S. G. Alikhanov, A. I. Alinovskii, G. G. Dolgov-Savel'ev, V. G. Eselevich, R. Kh. Kurtmullaev, V. K. Malinovskii, Yu. E. Nesterikhin, V. I. Pil'skii, R. Z. Sagdeev and V. N. Semenov, III Intern. Conf. on Plasma Physics, Novosibirsk, 1968, paper 24/A.

Translated by R. T. Beyer

On the constancy of an adiabatic invariant when the nature of the motion changes

A. V. Timofeev

(Submitted 28 April 1978)

Zh. Eksp. Teor. Fiz. 75, 1303-1308 (October 1978)

The motion of a charged particle in a spatially periodic field with amplitude increasing with the time is considered. The change of an adiabatic invariant when the particle is captured by a wave is calculated. The expressions obtained can also be used to describe the motion of a pendulum of variable length in a gravitational field as it goes from rotation to vibration about a position of stable equilibrium.

PACS numbers: 41.70. + t

1. It is well known that the motion of mechanical systems with slowly changing parameters can be characterized by a quantity which is conserved to very high accuracy, an adiabatic invariant (cf., e.g., Ref. 1). This assertion holds both for finite and for infinite motions of the representative point on the phase surface. In many cases, however, it is necessary to trace the transition from one type of motion to the other. For example, charged particles moving in a spatially periodic field whose amplitude increases with time can be captured by a wave. When this happens the trajectories on the phase surface go from the domain of infinite

motions to that of finite motions (see, e.g., Ref. 2). This problem has a simple mechanical analog, the motion of a pendulum of variable length in a gravitational field; here vibrations of the pendulum relative to a position of equilibrium correspond to finite motion, and rotations around the point of support, to infinite motion.

Besides these problems there are a number of others whose solution requires an analysis of the transition from one type of motion to another. In particular, there are certain problems of celestial mechanics (see,